

## Toxicology Research

Paper

# Mechanism of simulated lunar dust-induced lung injury in rats based on transcriptomics

Chen Gu<sup>1</sup>, Yan Sun<sup>2,\*</sup>, Meiqi Mao<sup>1</sup>, Jinguo Liu<sup>3</sup>, Xiongyao Li<sup>4</sup>, Xiaoping Zhang<sup>5</sup>

- <sup>1</sup>College of Basic Medical Sciences, Shenyang Medical College, Huanghe North Street 146, Shenyang 110034, China,
- <sup>2</sup>School of Pharmacy, Shenyang Medical College, Huanghe North Street 146, Shenyang 110034, China,
- State Key Laboratory of Robotics, Shenyang Institute of Automation, Chinese Academy of Sciences, Nanta Street 114, Shenyang 110016, China,
- 4Center for Lunar and Planetary Sciences, Institute of Geochemistry, Chinese Academy of Sciences, Lincheng West Road 99, Guiyang 550081, China,
- 5 State Key Laboratory of Lunar and Planetary Sciences, Macau University of Science and Technology, Weilong Road, Taipa, Macau 999078, China

Lunar dust particles are an environmental threat to lunar astronauts, and inhalation of lunar dust can cause lung damage. The current study explored the mechanism of lunar dust simulant (CLDS-i) inducing inflammatory pulmonary injury. Wistar rats were exposed to CLDS-i for 4 h/d and 7d/week for 4 weeks. Pathological results showed that a large number of inflammatory cells gathered and infiltrated in the lung tissues of the simulated lunar dust group, and the alveolar structures were destroyed. Transcriptome analysis confirmed that CLDS-i was mainly involved in the regulation of activation and differentiation of immune inflammatory cells, activated signaling pathways related to inflammatory diseases, and promoted the occurrence and development of inflammatory injury in the lung. Combined with metabolomics analysis, the results of joint analysis of omics were found that the genes Kmo, Kynu, Nos3, Arg1 and Adh7 were involved in the regulation of amino acid metabolism in rat lung tissues, and these genes might be the key targets for the treatment of amino acid metabolic diseases. In addition, the imbalance of amino acid metabolism might be related to the activation of nuclear factor kappaB (NF-κB) signaling pathway. The results of quantitative real-time polymerase chain reaction and Western blot further confirmed that CLDS-i may promote the occurrence and development of lung inflammation and lead to abnormal amino acid metabolism by activating the B cell activation factor (BAFF)/ B cell activation factor receptor (BAFFR)-mediated NF-κB signaling pathway.

Key words: lunar dust; transcriptome sequencing; differentially expressed genes; pulmonary toxicity mechanism; NF-kB signaling

#### Introduction

In recent years, human scientific research on the moon has become the trend and hotspot of deep space exploration in domestic and foreign space activities. Among the harsh and complex environmental factors on the lunar surface, long-term low gravity or microgravity, radiation exposure, and lunar dust and the dust particle environment formed by it still affect astronauts, and solving the impact of lunar dust on lunar exploration activities is one of the problems that must be solved for humans to return to the moon.1

It has been reported in the literature that the toxicological effects of lunar dust are highly dependent on the persistence of dust in the lungs, and its persistence is related to particle size, particle morphology, mineral and chemical composition, electromagnetic properties, concentration and exposure time, and cytotoxicity to macrophages.<sup>2</sup> About 20% of the lunar dust particles have a particle size smaller than 20  $\mu$ m, and 1%-2% of the fine dust particles have a particle size smaller than 3  $\mu m.^3$  The main constituents are pyroxene, plagioclase, glass-rich impact particles (cementitic glass), olivine and ilmenite.<sup>4</sup> Studies have shown that inhalation of lunar dust containing olivine, which can precipitate secondary minerals with a fibrous crystal structure that have the potential to induce harmful health effects similar to asbestos exposure.<sup>5</sup> Among the health effects of lunar dust on human body, the biggest threat is its harm to the respiratory system, which mainly comes from the inhalable particles. In particular, particles with a diameter of less than 2  $\mu$ m can evade the defense mechanism of the upper respiratory tract, reach the lower respiratory tract and alveoli, undergo gas exchange, and then enter the blood circulation, thereby causing damage to the respiratory system and circulatory system, and may even induce cancer.<sup>6</sup> In 1982, some researchers used the tracheal instillation method to change the exposure time of rats in the lunar soil suspension and found that the pathological process of the lungs developed in the form of an inflammatory response. Sun et al. 8 also confirmed this in the acute injury study of simulated lunar dust exposure to rat lung tissue, and their pathological results showed that its pulmonary toxicity was greater than that of PM2.5, and the severity was related to exposure time and dose. However, the underlying mechanism of simulated lunar dust-induced lung injury has not been clearly elucidated.

RNA sequencing (RNA-seq) is one of the high-throughput technologies to comprehensively analyze the transcriptomic changes, and to explore the potential molecular mechanisms through bioinformatics analysis.9 Transcriptomic technology is widely used in various fields, especially in the study of the toxicological mechanism of PM2.5. The researchers have performed RNA-seg on human umbilical vein endothelial cells

<sup>\*</sup>Corresponding author: School of Pharmacy, Shenyang Medical College, Shenyang 110034, China. Email: inksun@163.com; sunyan@symc.edu.cn

exposed to PM2.5. There were significant differential expressions of genes involved in stress, inflammation, and vascular dysfunction. Combined pathway analysis showed that these genes were involved in biological processes related to metabolism, inflammation, and host defense against environmental damage. This provides further insights into the underlying mechanisms of PM2.5-induced cardiovascular disease. 10 In addition, studies have shown that lungs exposed to different concentrations of PM2.5 have different transcriptional profiles.<sup>11</sup> As the concentration increased, PM2.5 induced more differentially expressed genes in lung tissue. Studies have results confirmed that gene-specific and genome-wide hypomethylation may be the main mechanism by which PM2.5 exacerbates lung diseases. 12 In addition, Liu et al. also found that PM2.5 exposure induced DNA damage by downregulating the expression of Beas-2B cells (Rad51), disrupting the DNA repair process and leading to genotoxicity of PM2.5.<sup>13</sup>

In previous toxicology studies of simulated lunar dust, the genome-wide transcriptional analysis of lung tissue exposed to simulated lunar dust was not clear, RNA-seq was used to analyze the mRNA expression profile of the transcriptome after exposure, and the biological functions, signaling pathways were analyzed Bioinformatics analysis of protein interaction networks. <sup>9</sup> This will provide us with new insights in the study of the mechanism of simulated lunar dust-induced lung injury. Therefore, this study infected rats with oral and nasal inhalation exposure systems, the lung tissue was removed for transcriptome sequencing. Combined with metabolomics analysis, the toxicity and mechanism of lung injury induced by simulated lunar dust in rats were studied.

## Materials and methods Preparation of simulated lunar dust suspension

The simulated lunar dust sample used in this study is lunar dust simulant (CLDS-i). The CLDS-i is as a gift from the Research Center of Lunar and Planetary Sciences, Institute of Geochemistry, Chinese Academy of Sciences. 14 It contains ~75 vol% glass and a little nanophase metal iron (np-Fe0), and with a median particle size about 500 nm. The CLDS-i particles also have complicated shapes and sharp edges, these properties are similar to those of lunar dust.  $^{15}$  Store at -80 °C for later use. When used, make up a certain concentration of suspension with normal saline.

#### Animal grouping and exposure

28 SPF male Wistar rats weighing 190 g ~ 220 g (Beijing Huafukang Biotechnology Co. Ltd, animal license number: SCXK [Jing] 2019-0008) were placed in polycarbonate cages (equipped with HEPA air filter), 2 animals/cage, 12 h-12 h light/dark cycle, room temperature: 24 °C  $\pm$  2 °C, relative humidity: 50%  $\pm$  5%, free food and water, reared for 1 week, and observed whether their activities and feeding were normal. Then weighed, and randomly divided into 2 groups: a simulated lunar dust-exposed group and a salineexposed group of 14-rats each.

The Wistar rats in the experimental group were placed in the oral and nasal exposure chamber (Beijing Huironghe Technology Co., Ltd) to be exposed to dust at a concentration of 7 mg/m<sup>3</sup> CLDS-i for 4 h/d, 7 d/week for 4 weeks, and the control group was under the same conditions exposure to saline. Rats were sacrificed one week after the last exposure for the next step of the experiment. Animal experiments were performed in accordance with the guidelines for animal experimentation of Shenyang Medical College, and all animal studies were approved by the Institutional Animal Research Ethics Committee.

## Generally

The mental state, fur color, diet, water intake, defecation and urination of the rats were observed every day, and the rats were weighed before, during and after the exposure, and their changes were recorded.

## Histopathological examination

The bilateral lung tissues (unwashed) of 4 rats in each group were taken, fixed with 10% paraformaldehyde solution, then dehydrated with ethanol gradient, xylene transparent treatment, lung tissues were embedded in paraffin, and then sliced at 5  $\mu$ m. Hematoxylin and Eosin (H&E) was used to observe the pathological changes of lung tissue.

## RNA sequencing

Part of the lung tissue of the remaining 5 rats in each group was taken, and total RNA was extracted with TRIzol reagent (Invitrogen, CA, USA). Oligo (dT) magnetic beads were used to enrich the mRNA with polyA structure in the total RNA. In this way, the mRNA is broken into fragments of about 300 bp in length. The mRNA is used as a template to synthesize the first strand of cDNA, and the first strand of cDNA is used as a template to synthesize the second strand of cDNA. Then, PCR amplification was used to enrich the library fragments, and then, the quality of the library was checked by the Agilent 2,100 Bioanalyzer, and then the total concentration of the library and the effective concentration of the library were detected. Libraries containing different Index sequences (adding different Index to each sample, and finally distinguishing the offline data of each sample according to the Index) were mixed in proportion. The pooled library was uniformly diluted to 2 nM and denatured by alkali to form a single-stranded library. After RNA extraction, purification, and library construction of the samples, the next-generation sequencing technology was used to perform paired-end sequencing on these libraries based on the Illumina sequencing platform.

#### Transcriptome bioinformatics analysis

First, the raw data (Raw Data) were filtered, and the highquality sequences (Clean Data) obtained after filtering were aligned to the reference genome of the species. According to the comparison results, the expression level of each gene was calculated. On this basis, we used DESeq to perform differential analysis of gene expression, and the conditions for screening differentially expressed genes were: expression difference fold |log2FoldChange| > 1, significant P-value<0.05, significant P-value<0.05. The differential genes were visualized by volcano plot and cluster analysis. Then, Gene Ontology (GO)/ Kyoto Encyclopedia of Genes and Genomes (KEGG) functional annotation and enrichment analysis were performed on the differential genes. GO annotation and enrichment analysis were applied to evaluate the biological function of differentially expressed genes (DEGs) and distribution in GO categories. KEGG pathway annotation and enrichment analysis were conducted to screen the most important signal transduction pathways involved

#### Metabolomics research

Lung tissues of rats treated with saline (n = 5) or CLDS-i (n = 5)were collected. After homogenizing, and disposing in 400  $\mu$ L of pre-cooled methanol/acetonitrile/water solution (4:4:2, v/v) at -20 °C for 60 min, the samples were centrifuged at 14,000 g for 20 min at 4 °C. The supernatant was collected and vacuum

**Table 1.** The forward and reverse primers used in this study.

Gene names	Forward primers	Reverse primers
CD19	ATGTGGGTTTGGGGGTCTC	AGGGTCGGTCATTCGCTTC
Cxcl13	CCTTGCAAAAATCAGGCTTCC	CACCTTAGGCTGGTAATGCGTC
BTK	CAGCACCAATCTCCACAAGT	AAATACTCCTCGCCCTTTCG
Cxcr5	GAAGGCAGAGAAAGGTGAGACT	GACTCTGCAATCACCCTCCC
Ccl19	TAACGATGCGGAAGACTGCT	CTGGTAGCCCCTTAGTGTGG
BAFF	CCGGAGGAAACAGTCATTCA	GCAAAGATGGGGTCCGTGTA
BAFFR	GGTCAAGCCATCAGGACCAA	CAGCTCTTCAGGTTCGAGGG
TRAF2	CGAAGACCGTTGGGGCTTT	CTGCAGGCTGAACACAGGTA
NIK	CCGCTCTGTCTCAAGATTGC	ACCTCCCACTTCCTGTAACG
P52	GAGGCCAAGGAGCTGAAGAAAGTCA	GGCAGGGAGAAGGAGCCATCACTAGC
GAPDH	GTATCGGACGCCTGGTTA	CATTTGATGTTAGCGGGAT
$\beta$ -actin	TACAACCTCCTTGCAGCTCC	GGATCTTCATGAGGTAGTCTGTC

dried, and 100  $\mu$ L of acetonitrile aqueous solution (acetonitrile: water = 1:1, v/v) was added for reconstitution during mass spectrometry analysis. After centrifuging at 14,000 g at 4 °C for 15 min, 2  $\mu$ L of the supernatant was used for ultra-high performance liquid chromatography-mass spectrometry (UPLC-MS, Thermo Fisher Scientific, USA) analysis.

The UPLC-MS data was processed using Compound Discoverer 3.2 (Thermo Fisher Scientific, USA) software with the specific parameters: mass ranged 70-1,050 m/z, peaks finding method centWave, mass tolerance 10 ppm, and retention time width threshold 40s, followed by unsupervising principal component analysis, supervising partial least squares discriminant analysis and orthogonal partial least squares discriminant analysis using the SIMCA-P 14.1 software (Umetrics, Umea, Sweden). Differential metabolites were identified via a screen criteria of P-value<0.05 and VIP > 1. These significant metabolites were visualized using volcano, column, and heat maps. 16 Furthermore, pathway enrichment analysis was performed using KEGG.

## RNA extraction and quantitative real-time polymerase chain reaction (qRT-PCR)

Total RNA was extracted from the remaining frozen lung tissues with TRIzol reagent (Vazyme, China) according to the manufacturer's instructions. The isolated RNA was converted into cDNA using HiScript II QRT SuperMix for qRT-PCR (+gDNA wiper) reverse transcription reagent (Vazyme, China) according to the manufacturer's instructions. qRT-PCR reactions were performed using SYBR GreenPCR Master Mix (Vazyme, China) on an ABI PRISM 7,500 system. The mRNA levels of gene CD19, Chemokine ligand13 (Cxcl13), Bruton tyrosine kinase (BTK), Chemokine receptor5 (Cxcr5), Chemokine ligand 19 (Ccl19), B cell activation factor (BAFF), B cell activation factor receptor (BAFFR), Tumornecrosis factor receptor-associated factor 2 (TRAF2), nuclear factor kappaB (NF-κB)-inducing kinase (NIK) and P52 were measured by gRT-PCR. The forward primers and reverse primers (Invitrogen, CA, USA) were summarized in Table 1. For BTK, glyceraldehyde-3-phosphate dehydrogenase (GAPDH) was selected as the internal reference gene, and for CD19, Ccl19, Cxcr5, Cxcl13, BAFF, BAFFR, TRAF2, NIK and P52, the housekeeping gene  $\beta$ -actin was selected as the internal reference gene. The data of the tested genes were analyzed using the  $2^{-\Delta\Delta CT}$  method.

#### Western blotting analysis

The remaining lung tissues were homogenized with RIPA protein lysate (containing 1 mM PMSF) (Wanleibio, Liaoning, China). Then, the homogenate was centrifuged at 12,000 g, at 4 °C for 30 min and the supernatant was collected. Subsequently, protein levels were estimated by the Bradford protein assay (Bio-Rad Hercules, CA, USA). Total proteins were electrophoresed in a SDS-PAGE system, and the gel bands were electrophoretically transferred to polyvinylidene fluoride membranes. The membranes were blocked with 5% skim milk for 1 h. Using BAFFR, TRAF2, P52, NIK, IL-1 $\beta$ , BAFF, TNF- $\alpha$  and GAPDH (Wanleibio, Liaoning, China) and  $\beta$ -actin (Santa Cruz Biotechnology, Santa Cruz, CA) antibodies were immunoblotted at the manufacturer's recommended dilution. Protein signals were finally detected using enhanced chemiluminescence reagent (Wanleibio, Liaoning, China).

## Statistical analysis

All data were analyzed by SPSS 20.0 statistical software and expressed as mean  $\pm$  SD. Student's t-Test was used in analysis between two groups. All of the mRNA and protein expression were analyzed using one-way ANOVA. And the correlation heat map analysis and network analysis of the differential genes and differential amino acid metabolites were performed using the "spearman" algorithm and Cytoscape 3.3.0 software. P < 0.05 was defined as a statistically significant difference.

#### Results

#### Lung histopathological observation

H&E staining showed that lung structures in the normal saline group were basically normal, and there were a small number of red blood cells in the alveolar wall. The pathological changes of lung tissues in CLDS-igroup were obvious, with a large number of red blood cells in the alveolar wall and alveolar cavity, severe congestion, a large number of inflammatory cells aggregation and infiltration, and thickening of the lung septum. The alveolar structures were altered, the basic lung structures were not clear and could not be distinguished, and the rupture was severe (Fig. 1).

#### Symptoms of rats during the experiment

Before modeling, all rats were generally in good growth condition, with consistent weight gain, white hair, smooth and shiny, active and responsive, with normal diet and water. In CLDS-i group, the rats were lethargic, obviously emaciated, cough symptoms, yellow and coarse coat color, reduced activity, and poor sensitivity to external reactions than before modeling. In CLDS-i group, urine was more than before, and there was obvious urine accumulation

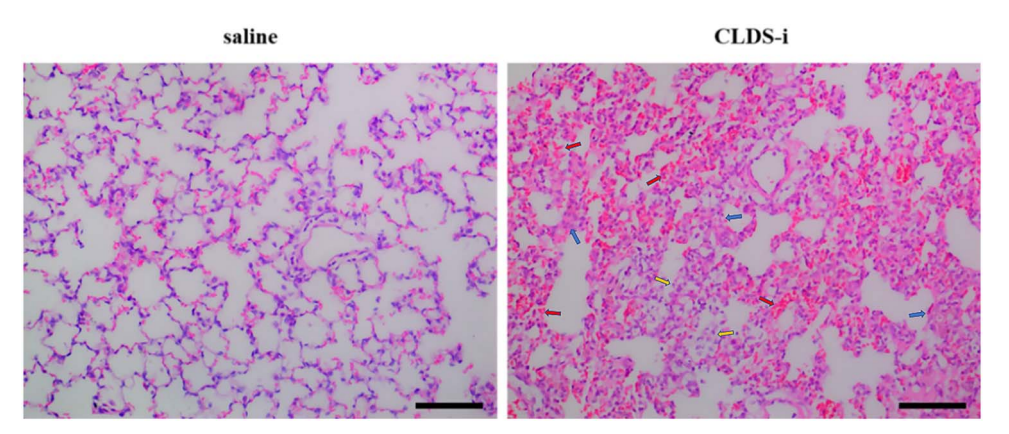


Fig. 1. Hematoxylin-eosin-stained histopathological pictures of rat lungs. Arrows indicate inflammatory cells, congestion, and septal widening, respectively. Original magnification  $\times$  200; scale bar = 100  $\mu$ m.

**Table 2.** Effects of CLDS-i exposure on feed intake in rats (n = 5,  $x^- \pm s$ ; g).

Group	saline	CLDS-i
1 week	$22.57 \pm 0.53$ g	19.37 ± 0.23 g***
2 weeks	$23.91 \pm 0.29 \mathrm{g}$	17.83 ± 0.40 g*
3 weeks	$21.97 \pm 0.31 \mathrm{g}$	$21.2 \pm 0.28 \mathrm{g}$
4 weeks	$20.71 \pm 0.15 \text{ g}$	$18.18 \pm 0.35 \mathrm{g}^{***}$

Note: Compared with saline group.  $^{*}P < 0.05$ .  $^{***}P < 0.001$ .

**Table 3.** Effects of CLDS-i exposure on water intake in rats (n = 5,  $x^- \pm s$ ; mL).

Group	saline	CLDS-i	
1 week	$33.97 \pm 1.57  \text{mL}$	$40.43 \pm 2.55 \text{ mL}$	
2 weeks	$33.60 \pm 1.40 \text{ mL}$	$43.06 \pm 1.65 \text{ mL}$	
3 weeks	$26.80 \pm 1.04  \text{mL}$	$32.34 \pm 1.59 \text{ mL*}$	
4 weeks	$22.62 \pm 0.41 \text{ mL}$	$22.44 \pm 0.60 \text{ mL}$	

Note: Compared with saline group.  $^{*}P < 0.05$ .

in the bedding material. Compared with before modeling, the diet and water intake of rats in the two groups increased first and then decreased, but the changes were more obvious in the CLDS-i group than in the saline group (Tables 2 and 3, Fig. 2A-C).

## Comparison of body mass and lung mass in each group

The results in Fig. 3 and Table 4 showed that there was no significant difference in body weight between the two groups in the first week (P > 0.05). The second week of exposure, the body weight of rats in CLDS-i group was significantly lower than that in the saline group (P < 0.05). At the third and fourth weeks, the weight of rats in CLDS-i group increased slowly, which was significantly lower than that in saline group (P < 0.001), indicating that compared with saline group, the weight of rats in CLDS-i group showed significant wasting symptoms. Furthermore, we have detected the weight of lungs which were wet or dry. The results showed the wet and dry lungs in the CLDS-I group were both heavier than those in the saline group (Table 5).

## Transcriptome analyses

In order to investigate the molecular mechanism of lung injury induced by simulated lunar dust particles in rats, RNAsequencing was performed to analyze changes in genomewide expression profiles in CLDS-i-exposed lung tissues. The data were shown in Fig. 4A, with the multiple of expression difference |log2FoldChange| > 1 and significant P-value<0.05 as the screening criteria, a total of 571 differentially expressed genes were identified between the two groups. Compared with the saline group, in the CLDS-i group, 381 genes were up-regulated, while 190 genes were down-regulated. And the fold changes of DEGs were visualized by volcano plots (Fig. 4B). Cluster analysis was used to judge the expression patterns of differentially expressed genes under different experimental conditions. Rows indicated gene types, columns indicated sample types, red indicated highly expressed genes, and green indicated low expressed genes. As shown in Fig. 4C, compared with the saline group, most DEGs were up-regulated in lung tissues of CLDS-i group.

The differential genes were enriched into the GO database, GO classification was performed according to molecular function (MF), cellular component (CC) and biological process (BP), and the top 10 GO term items with the P < 0.05 in each GO classification were selected (Fig. 5). GO category analysis showed that differential genes were significantly enriched in immune receptor activity, cytokine receptor activity, cytokine receptor binding and chemokine receptor activity in MF, and immune response and regulation of immune system process, activation and differentiation leukocytes, lymphocyte activation and so on in BP. According to the GO enrichment results, the degree of enrichment is measured by rich factor, false discovery rate (FDR) and the number of genes enriched on this GO term, and the top 20 GO term entries with FDR < 0.05 were selected, that is, the most significant enrichment (Fig. 6). The analysis of the results showed that CLDS-i was involved in the activation and differentiation of immune cells,

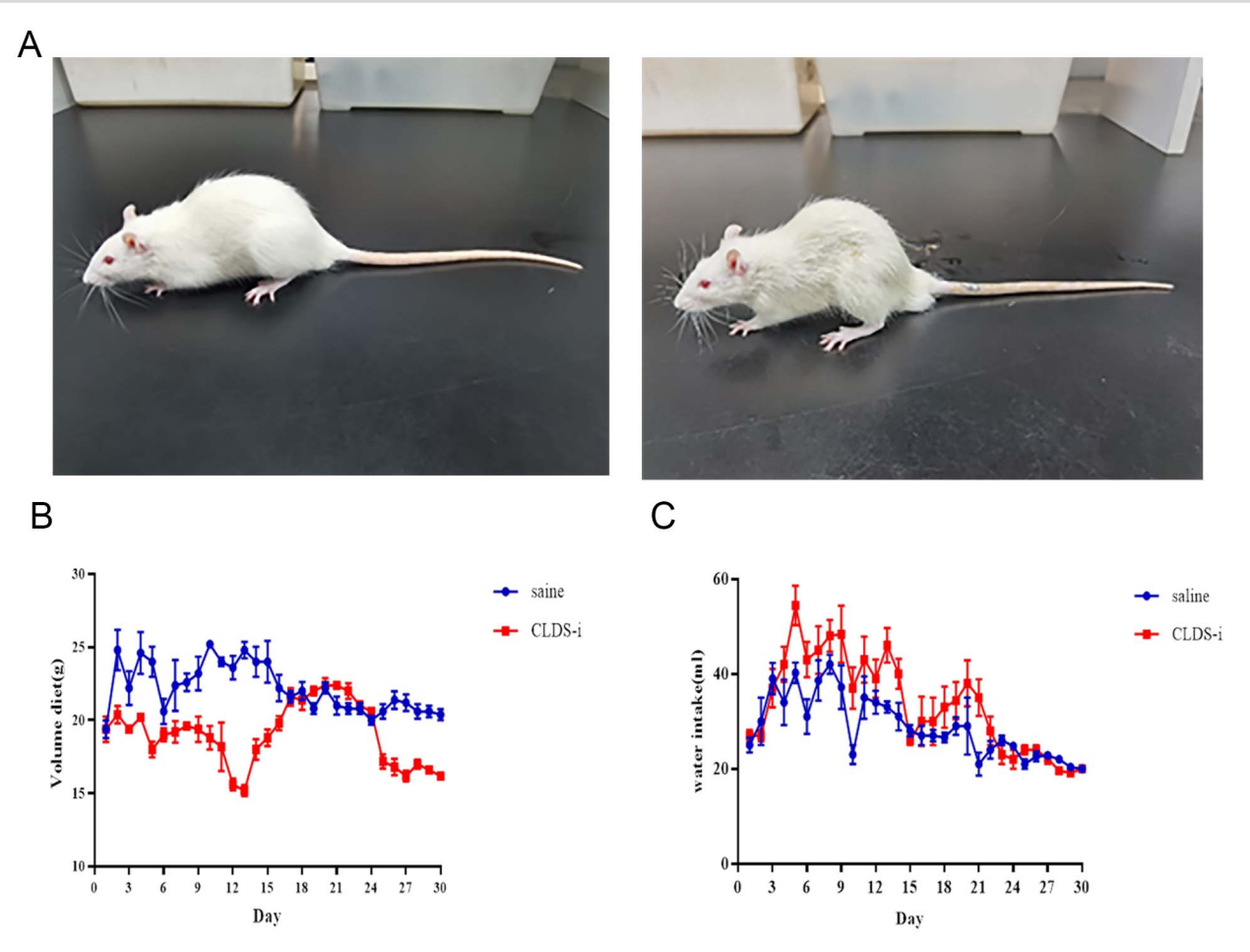


Fig. 2. Changes of diet and water intake of rats in two groups. A) The photos of rats in saline and CLDS-i groups. B) Effects of CLDS-i exposure on feed intake in rats (n = 5,  $x^- \pm s$ ; g). C) Effects of CLDS-i exposure on water intake in rats (n = 5,  $x^- \pm s$ ; mL).

**Table 4.** Changes in body weight of rats in each group (n = 5,  $x^- \pm s$ ; g).

Group	saline	CLDS-i	
1 week	$241.13 \pm 28.84$	235.60 ± 25.59	
2 weeks	$336.67 \pm 30.18$	$313.07 \pm 23.45^*$	
3 weeks	$404.73 \pm 23.81$	374.67 ± 16.03***	
4 weeks	$443.2 \pm 22.37$	$403.90 \pm 15.79$ ***	

Note: Compared with saline group \*P < 0.05. \*\*\*P < 0.001.

**Table 5.** The weight of lungs in each group (n = 5,  $x^- \pm s$ ; g).

F	F	F	
Lung wet weight	$1.72 \pm 0.10$	$1.82 \pm 0.14$	
Lung dry weight	$0.30 \pm 0.01$	$0.45 \pm 0.02**$	

Note: Compared with saline group. \*P < 0.05. \*\*P < 0.001.

which disturbed the regulation of immune system responses and promoted the occurrence of inflammation.

These differential genes were aligned to the KEGG database, and as shown in Fig. 7, with P < 0.05 as the screening criterion, the top 30 KEGG pathways were selected. According to KEGG function annotation analysis, the pathways were significantly enriched in the "organismal systems and human diseases". According to the KEGG enrichment results, select the top 20 KEGG pathways with the smallest FDR value (FDR generally ranges from 0 to 1, the closer it is to zero, the more significant the enrichment is) (Fig. 8A). The results showed that most of its signaling pathways were

related to inflammation and disease, indicating that the inflammation and disease-related signaling pathways in the lung tissue of rats exposed to CLDS-i were significantly activated. At the same time, we used Cytoscape software to conduct network analysis on the pathways enriched in genes related to inflammatory diseases, as shown in Fig. 8B. The results showed that the same gene was involved in multiple signaling pathways at the same time.

## Confirmation of RNA-Seq data by qRT-PCR

Through GO and KEGG database analysis, it was shown that CLDSi significantly affected the inflammation and disease-related

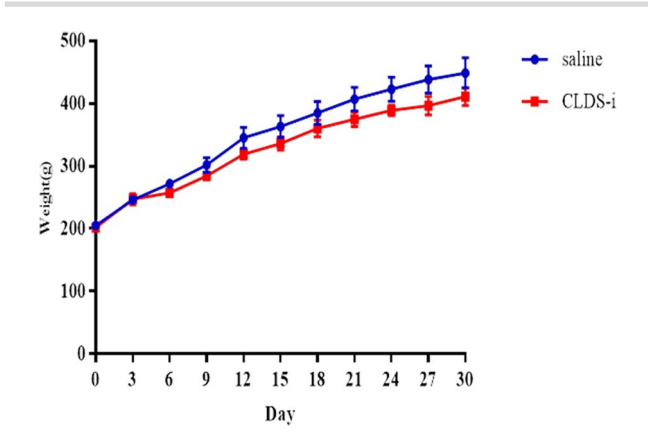


**Fig. 3.** Changes in body weight of rats in each group (n = 5,  $x^- \pm s$ ; g).

signaling pathways in rat lung tissue. In order to verify the sequencing results, several related genes in inflammation-related signaling pathways were selected: CD19, Cxcl13, BTKCxcr5 and Ccl19 and primers were designed.  $\beta$ -actin and GAPDH as internal controls to verify at the mRNA level. The results of qRT-PCR experiments showed that, the expression of these inflammationrelated genes was consistent with the transcriptome sequencing results. Compared with the saline group, the expression of these genes was significantly up-regulated in the CLDS-i group, as shown in Fig. 9A.

## Conjoint analysis

In the previous metabolomics research results of simulated lunar dust induced lung injury in rats, it was found that simulated lunar dust exposure disrupted the amino acid metabolism, lipid metabolism, carbohydrate and nucleotide metabolism balance in the lung tissue of rats. Combined with KEGG metabolic pathway analysis, it was found that the amino acid metabolism had the greatest impact. In order to explore the relationship between differential genes and differential amino acid metabolites in simulated lunar dust group and normal saline group, a joint analysis was conducted, the "spearman" algorithm and Cytoscape 3.3.0 software were used for the correlation heat map analysis and network analysis of differential genes and differential amino acid metabolites. The results were shown in Figs 9B and 10.

As can be seen from Fig. 9B, there were five genes involved in amino acid metabolism. These were ENSRNOG00000003709 (Kynurenine 3-monooxygenase, Kmo), ENSRNOG00000029993 (Kynureninase, Kynu), ENSRNOG00000009348 (nitric oxide synthase 3, Nos3), ENSRNOG00000013304 (argininase-1, Arg1) and ENSRNOG00000032959 (Adh7). Each gene had a different association with a variety of amino acid metabolites. As shown in Fig. 10, Kmo was positively correlated with L-Proline, Argininosuccinic.acid and (E)-p-coumaric. Acid; It was negatively associated with L-(-)-threonine, Taurine and PHENYLACETAMIDE. Kynu was positively correlated with Argininosuccinic.acid, L-Proline and (E)-p-coumaric. Acid; It was negatively correlated with D-PANTOTHENIC ACID and Taurine. Nos3 was positively correlated with L-Histidine, L-Hydr-oxyproline, L-Tyrosine and 3-(3,4-dihydroxypropanoic. Acid; It was negatively correlated with L-Phenylalanine. Arg1 was positively correlated with Lhydroxyproline, l-histidine, N6, N6, N6-trimethyl-L-lysine, L-(-)methionine and PHENYLACETAMIDE; It was negatively correlated with 3-Ureidopropionic acid. Adh7 was positively correlated with Taurine and L-Hydroxyproline; It was negatively correlated with L-Proline, (E)-p-coumaric. Acid and 3-Ureidopropionic.acid.

Then we combined KEGG database analysis and found that under the regulation of Kmo, Arg1, Kynu and other genes, simulated lunar dust exposure affected tryptophan metabolism, arginine and proline metabolism, arginine biosynthesis, amino acid biosynthesis, and tyrosine metabolism pathways in rat lung tissue. At the same time, the levels of glutamic acid, proline, spermidine, statin, histidine and other metabolites decreased. After comparison, the up regulation and down regulation of differentially amino acid metabolites and differentially expressed genes as well as their participation in related pathways were shown in Table 6.

## The effect of CLDS-i on the expression of genes and proteins related to NF- $\kappa$ B signaling pathway

Previous studies have shown that abnormal amino acid metabolism is closely related to inflammatory response. It has been proven that threonine can inhibit the activity of NF-κB and the expression of cytokines to prevent lung injury.<sup>17</sup> The study on the mechanism of amino acid catabolism in human hepatocytes showed that mTORC1 regulates expression of aspartate aminotransferase, glutamate dehydrogenase, glutamic acid decarboxylase and ornithine decarboxylase genes by NF- $\kappa$ B to control the utilization of glutamic acid and ornithine by hepatocytes. 18 In addition, the effects of glutamine, leucine and proline on inflammation and insulin sensitivity markers in HepG2 hepatocytes were studied. It was found that glutamine, leucine and proline may reduce IL- $1\beta$ -stimulated inflammatory response by inhibiting NF- $\kappa$ B, and that they might be able to regulate insulin signaling in HepG2 hepatocyte model. 19 These results indicate that abnormal amino acid metabolism is closely related to the activation of NF- $\kappa$ B signaling pathway.

To explore the effect of CLDS-i exposure on NF-κB signaling pathway in rat lung tissue. We detected the expression levels of related genes and proteins in this pathway. The results were shown in Fig. 11. Compared with the saline group, the mRNA levels of BAFF, BAFFR, TRAF2, NIK and P52 were increased in the CLDS-i group, and these changes are also showed in protein expression.

#### Discussion

Previous studies have shown that the inflammatory response induced by lunar dust exposure is an extremely important mechanism leading to pulmonary fibrosis. However, its potential toxicity mechanism is still unclear.

Because real lunar dust samples are very scarce, they are very precious. A large number of literature shows that researchers at home and abroad usually use simulated lunar dust to carry out various ground tests and experimental verifications, as well as lunar dust biological toxicity studies. For example, the National Aeronautics and Space Administration and European Space Agency engineers and scientists have used JSC-1A (ground volcanic ash from Merriam Crater in San Francisco, Arizona) as lunar dust substitutes, which are applied for various lunarrelated test studies.<sup>20-22</sup> There are also MKS-1 and FJK-1 simulated lunar dust samples from Japan, and CAS-1 developed by China (developed from the Jinlongdingzi volcanic eruption of the Longgang volcanic group in the Changbai Mountains in northeastern China). 15,23 In this study, the simulated lunar dust sample we used is CLDS-i, which is also one of a series of simulated lunar dust samples.8 CLDS-i has an average grain size of about 500 nm, a complex shape with sharp edges and contains ~75 volume (vol)% glass and ~15 vol% plagioclase, and

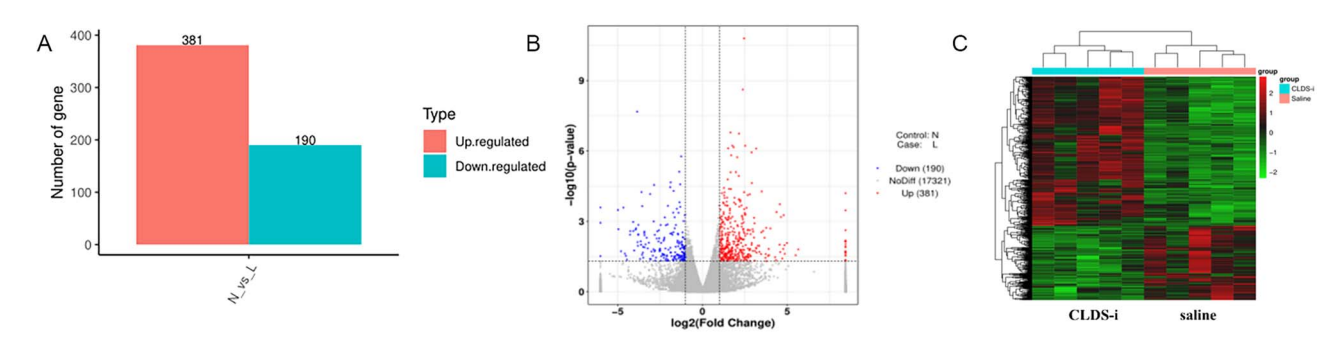


Fig. 4. Analysis of differentially expressed genes between normal saline and CLDS-i-exposed lungs. A) The number of up-regulated and down-regulated differential genes between CLDS-i-exposed lungs and saline-exposed lungs. B) The folds of differential genes were visualized by volcano plots. C) Heatmap of 571 differentially expressed genes between the two groups.

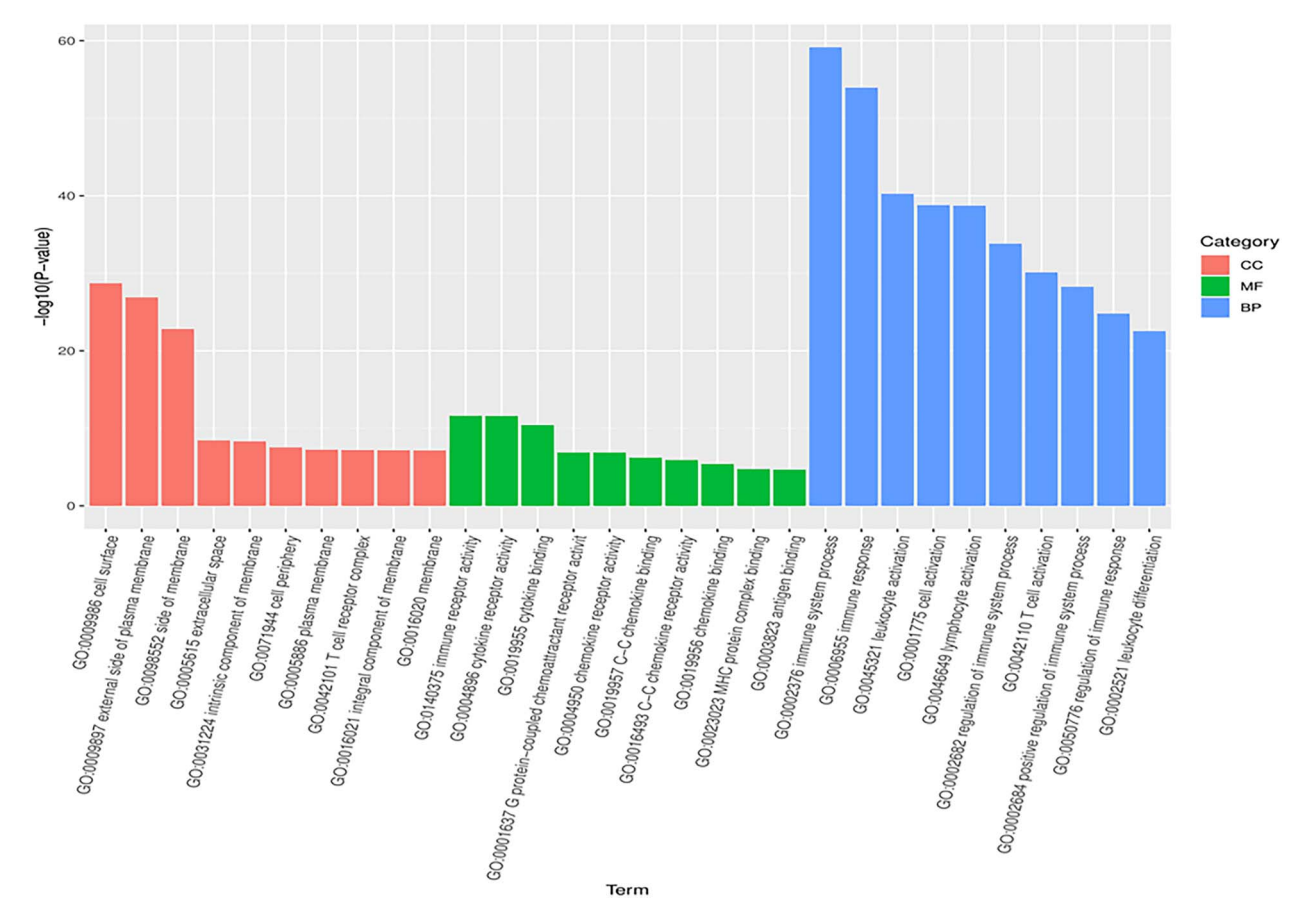


Fig. 5. The functional enrichment analysis of differential genes after GO analysis. The 571 differential genes were divided into three categories in the  $\overrightarrow{GO}$  annotation. In each GO category, the top 10 GO term items with P < 0.05. BP, biological process; CC, cellular component; MF, molecular function. The X -axis shows the different GO items and the Y-axis is the -log10 (P-value) enriched for each term.

Table 6. Summary table of the results of combined transcriptomics and metabolomics analysis of the simulated lunar dust group vs the saline group.

Related pathways	Differentially expressed genes	Differential metabolites
Tryptophan metabolism	Kmo√Kynu (↑)	Skatole Indole (\psi)
Arginine and proline metabolism	Arg1、Nos3 (↓)	Glutamate、Proline、Spermidine (↓)
Arginine biosynthesis	Arg1、Nos3 (↓)	Glutamate、L-Arginosuccinate (↓)
Biosynthesis of amino acids	-	Histidine、Tyrosine、Phenylalanine、Leucine、Asparagine、Proline (↓)
Tyrosine metabolism	Adh7 (↓)	4-Coumarate、Tyrosine、3,4-Dihydroxy-phenylpropanoate (\u00e4)

 $\sim$ 10 vol% olivine, pyroxene and titanium Iron ore, in addition, it contains np-Fe0 particles. 15 It is similar to real lunar dust in phase composition, chemical composition, particle size and shape and properties of nano-metal iron. Therefore, CLDS-i can be applied in many fields such as scientific research of lunar dust, processing technology and toxicology research. 15

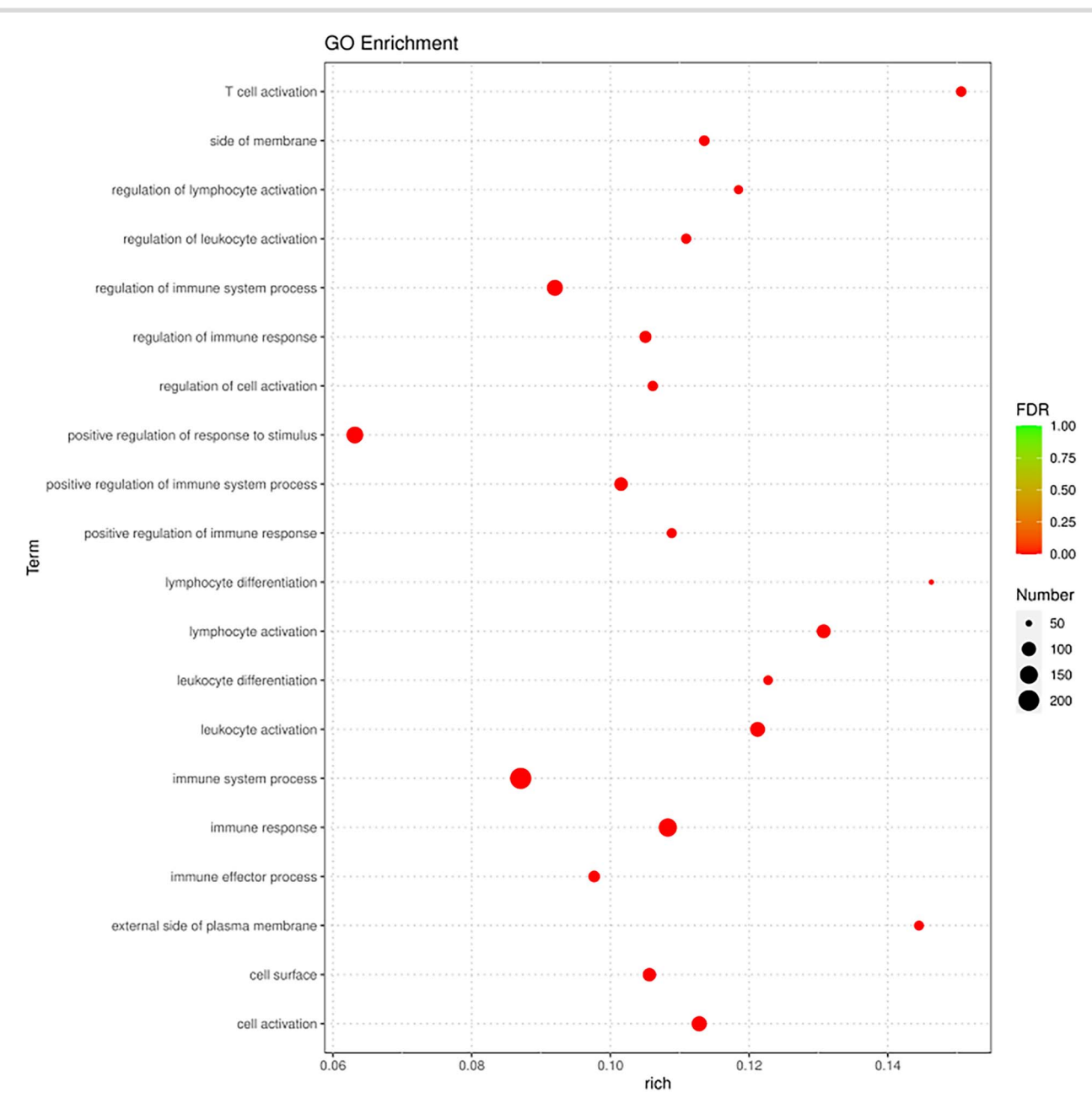


Fig. 6. The top 20 GO term with the most significant enrichment in the GO functional annotations of differential genes between the two groups were displayed. Rich factor refers to the ratio of the number of enriched differential genes to the number of annotated genes in the GO term. The greater the rich factor, the greater the degree of enrichment. FDR generally ranges from 0 to 1, and the closer it is to zero, the more significant the enrichment is.

In the previous lunar dust toxicology studies, the tracheal instillation method was mostly used in animal exposure model for particulate matter exposure, but the tracheal instillation method had limitations. In this way, animals are not exposed to natural air breathing conditions. And in the experiments, we found that this method is easy to cause mechanical damage to the trachea and high mortality in animals. Therefore, it is not suitable to carry out longer-term infusion exposure experiments. In recent years, the whole body exposure system and the oral and nasal exposure system have gradually emerged. The toxic effects and mechanisms on the body are discussed by simulating the exposure of particulate matter. This method is more scientific and can more truly reflect the pathological process, which is in line with the actual particulate matter exposed the situation. This experiment

was carried out under a single-concentration oral-nose exposure

In the research of rats were inhaled at 6.8 mg/m<sup>3</sup> for 4 weeks. Pulmonary toxicity was reported on day 1, 1 week, 4 weeks and 13 weeks after inhalation exposure was terminated and found at any post-exposure assessment time Statistically significant differences were not observed for some toxicity biomarkers in the lungs of rats exposed to 6.8 mg/m<sup>3</sup> lunar dust, only to find a slight increase in bronchoalveolar lavage fluid neutrophils at 13 weeks. Therefore, 6.8 mg/m<sup>3</sup> was considered the highest no-obviously damaging effect level (NOAEL).24 Besides, we performed 3 doses of CLDS-i (2.1 mg, 6.3 mg, and 18.9 mg per rat) to induce pulmonary fibrosis in rats in our previous study.<sup>25</sup> The results showed that all of these 3 doses would induce pulmonary fibrosis and contribute

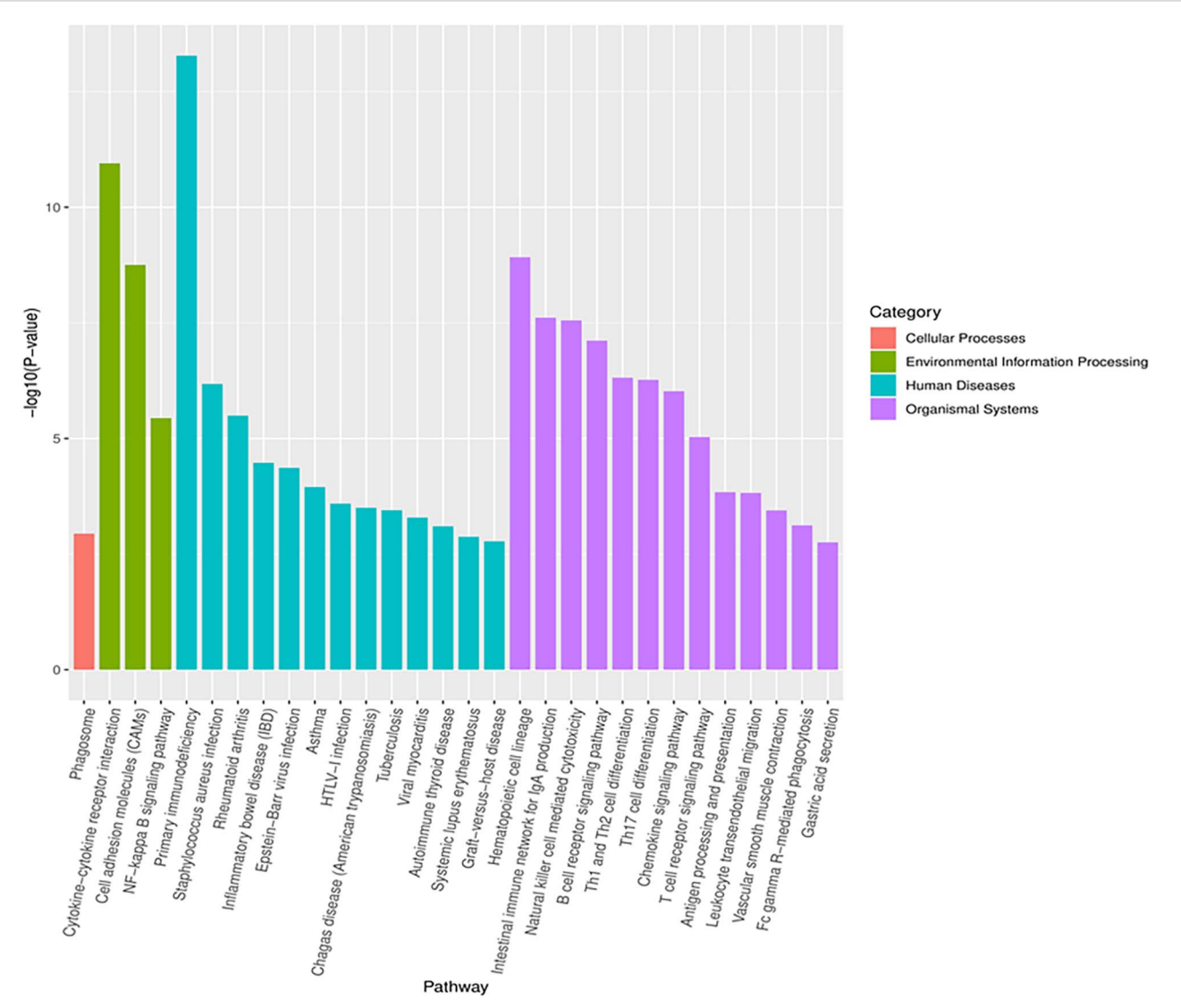


Fig. 7. KEGG classification of DEGs from normal saline group and CLDS-i group. The identified gene functions fall into four broad categories: cellular  $processes, environmental\ information\ processing, human\ disease\ and\ organismal\ system.$ 

to the inflammatory response. From the morphological results of lungs, dose between 6.3 mg and 18.9 mg per rat seemed suitable to further investigate the function of CLDS-i in rats. Because of the morphological structures of lungs in rats treated by 18.9 mg CLDSi were almost disappeared. The exposure condition of our current study was 7 mg/m<sup>3</sup> CLDS-i for 4 h/d, 7 d/week for 4 weeks. And the body weights of male rats were 190 g  $\sim$  220 g, which corresponded to rats aged from 2 to 3 months. The mean minute respiratory volume of male rats aged from 2 to 3 months is 228.36 mL/min to 266.83 mL/min.<sup>26</sup> So the total dose of CLDS-i used in our current study is 10.742 to 12.552 mg, which is between 6.3 mg and 18.9 mg. Since the dose setting in this experiment needs to cause at least mild pathological changes under the condition of not exceeding the lung load of rats, and then to study the molecular mechanism of pulmonary toxicity of simulated lunar dust particles, it is reasonable to set the dose concentration of 7 mg/m<sup>3</sup>.

In this study, we obtained a genome-wide transcriptional signature of lung tissue exposed to simulated lunar dust CLDS-i. The results confirmed that DEGs induced by CLDSi were mainly involved in the activation and differentiation of inflammatory immune cells. KEGG analysis showed that CLDS-i significantly activated signaling pathways related to inflammation and immune response. These pathways include: Inflammatory bowel disease, T cell receptor signaling pathway,  $NF-\kappa B$  signaling pathway, Rheumatoid arthritis (RA), Chemokine signaling pathway, Staphylococcus aureus infection, Th17 cell differentiation, Th1 and Th2 cell differentiation, B cell receptor signaling pathway, Cytokine-cytokine receptor interaction, primary immunodeficiency and so on.

In addition, we found that CLDS-i affected the balance of tryptophan metabolism, and under the regulation of Kmo and Kynu genes, the levels of tryptophan metabolites skatole and indole decreased. The expression product of Kmo is Kynurenine 3monooxygenase and the expression product of Kynu is Kynureninase. Kynurenine pathway (KP) is the main pathway of tryptophan catabolism in most mammalian cells. Kmo and Kynu are important key enzymes in KP.<sup>27</sup> Under inflammatory conditions, KP enzymes, specifically Kmo, are upregulated, increasing the production of toxic KP metabolites in the brain, Dysregulation of KP and increased levels of toxic metabolites are associated with the occurrence of many diseases, including neurological disorders, autoimmune related diseases RA, multiple sclerosis,

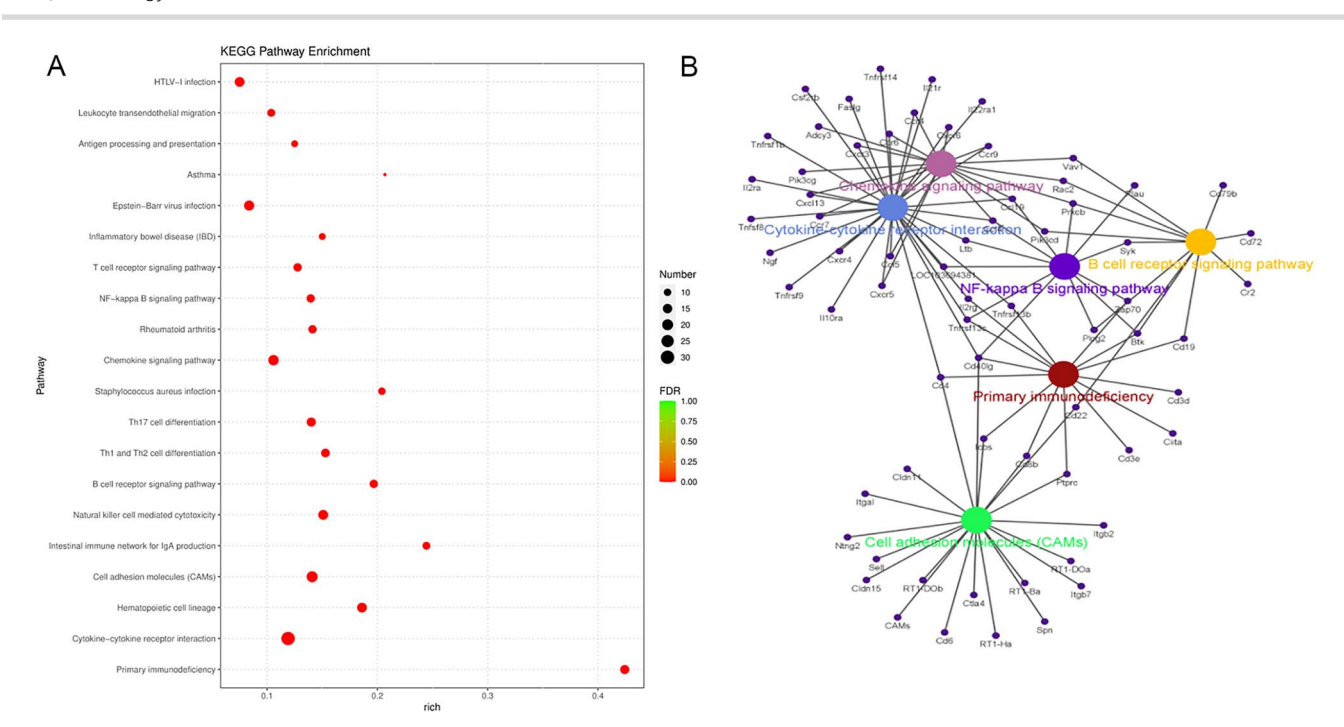


Fig. 8. KEGG enrichment analysis and interaction pathway network of selected genes. A) The scatter plot of the top 20 significantly enriched KEGG pathways for DEGs in the CLDS-i vs saline group. The Y-axis represents the different pathways and the X-axis represents the enrichment factors. The bubble size is represented by number, which represents the number of DEGs significantly enriched in the corresponding pathway. And the color is represented by FDR. Rich factor refers to the ratio of the number of enriched differential genes to the number of annotated genes in the pathway. The greater the rich factor, the greater the degree of enrichment. FDR generally ranges from 0 to 1, and the closer it is to zero, the more significant the enrichment is. B) the interactive pathway network of the genes determined by Cytoscape software.

cardiovascular disease, ischemic stroke and malignancies colorectal cancer.<sup>28</sup> In addition, in chronic inflammatory skin diseases such as psoriasis and atopic dermatitis, the tryptophan metabolizing enzyme Kynuis significantly up-regulated, and the expression level of Kynu is positively correlated with the severity of disease and inflammatory response.<sup>29</sup> Kmo and Kynu play an important role in a variety of inflammatory diseases in humans. The imbalance of tryptophan metabolism is closely related to the occurrence and development of inflammatory bowel disease (IBD). In the analysis of serum samples from patients with IBD, it was found that serum tryptophan level was negatively correlated with IBD activity, and tryptophan deficiency may lead to the development of IBD and increased disease activity.30 Colorectal cancer is a major complication in patients with long-term IBD, and targeted therapy targeting tryptophan metabolites may improve the success rate of treatment for IBD and colorectal cancer.<sup>31</sup>

CLDS-i also affected the metabolic pathway of arginine and proline as well as the biosynthetic pathway of arginine, and Glutamate, Proline, Spermidine and L-Arginosuccinate decreased under the regulation of Nos3 and Arg1 genes. Endothelial NOS3 is a subtype of nitric oxide synthase (NOS). Inducible nitric oxide synthase (iNOS) is another subtype. Nitric oxide synthesized by NOS plays a key role in regulating pulmonary vascular tension.<sup>32</sup> NOS3-derived NO has physiological effects on healthy lung function, while NO synthesized by iNOS has cytotoxic effects and causes lung injury.<sup>25,33</sup> Previous studies have shown that fine particle exposure can stimulate the release of protective NO in cells, up-regulate iNOS and down-regulate endothelial NOS, suggesting that fine particle exposure changes the NO/NOS system.34 Arginine is an essential nitrogen carrier for the synthesis of polyamines, prolines and other proteins, in which Arg1 plays a key role. Increasing Arg1 activity can promote L-arginine catabolism.

In addition, arginine plays an important role in the synthesis of endogenous nitric oxide. The L-arginine-No pathway exists in vascular endothelial cells, which catalyzes the production of NO under the activation of the Arg-NO pathway. NO can inhibit Th17related cytokines and synergistically increase the secretion of Glucagon-like peptide (GLP-1). GLP-1 also promotes nitric oxide production and has direct anti-inflammatory effects by inhibiting the NF- $\kappa$ B pathway.<sup>35</sup> We speculated that the simulated lunar dust would cause the disorder of arginine synthesis metabolism in lung tissue, which would not only affect the biosynthesis of ornithine, polyamine, proline and other amino acids, but also interfere with L-arginine-NO pathway, thus affecting the production of NO and causing the imbalance of NO in the body, leading to the occurrence of pneumonia. We also found lower levels of leucine, histidine and asparagine. Leucine, as a branched chain amino acid, is mainly involved in energy metabolism, and asparagine plays a role in intestinal mucosal immune barrier function.<sup>36</sup> Histidine can inhibit the expression of proinflammatory factors in adipocytes through NF- $\kappa$ B pathway and thus play an antiinflammatory role.37 Our results suggest that exposure to simulated lunar dust affects tricarboxylic acid cycling and energy consumption processes, disrupts immunomodulatory processes, and leads to pulmonary inflammation.

A large number of studies have confirmed that the metabolic disorder of amino acids is related to the activation of NF- $\kappa$ B signaling pathway. The NF- $\kappa$ B pathway is one of the most important cellular signal transduction pathways involved in physiological processes and disease states, and is involved in the control of immune function, inflammation, stress response, differentiation, apoptosis, and cell survival as well as it plays an important role in the development of cancer. In this study, the metabolic pathway with significant enrichment of differential genes involved NF- $\kappa$ B

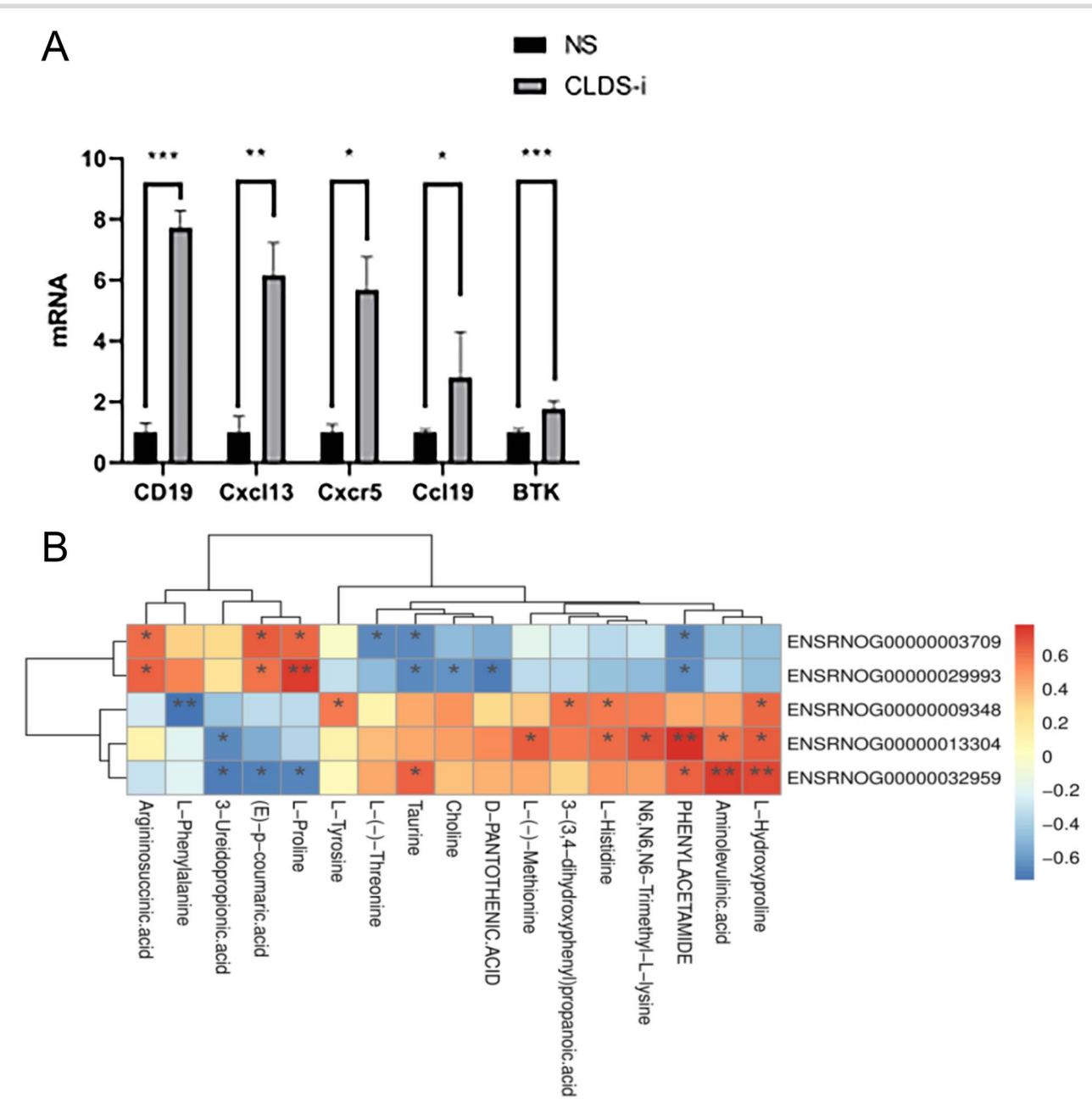


Fig. 9. A) CD19, Cxcl13, BTK, Cxcr5 and Ccl19 mRNA expression in rat lungs (n = 5). Data were presented as mean  $\pm$  standard deviation. Compared with the saline control group, \*P < 0.05, \*\*P < 0.01, \*\*\*P < 0.001. B) Heat map analysis of correlation between differential genes and amino acid  $metabolites. \ Note: The \ value \ range \ of \ correlation \ coefficient \ (corr) \ is \ (-1, +1). \ corr>0 \ indicates \ positive \ correlation. \ corr<0 \ indicates \ a \ negative$ correlation, and the larger absolute value, the greater correlation. corr = 0 indicates no correlation. P value reflects the significance level of correlation, and P value <0.05 indicates that the gene is significantly correlated with the metabolite. \*P < 0.05, \*\*P < 0.01, \*\*\*P < 0.001.

signaling pathway, and we speculated that the activation of NF- $\kappa$ B signaling pathway may be one of the main reasons why CLDSi induces lung injury, promotes inflammation, and disrupts the balance of amino acid metabolism.

In our experimental results, the expression level of TNF family BAFF in the lung tissues of rats in the simulated lunar dust group was significantly increased, and the mRNA and protein expression levels of BAFFR, the specific receptor for BAFF to regulate B cell survival, was also significantly up-regulated, suggesting that the abnormal expression of BAFF/BAFFR may be involved in the occurrence of pneumonia. BAFF plays a key role in B cell homeostasis, proliferation, maturation and survival action.  $^{39,40}$  BAFF has three receptors: BAFFR, transmembrane activator calcium ion signal

regulator cyclophilin ligand (TACI), B cell maturation antigen (BCMA). Among them, BAFFR plays a role in the development and maturation of immature B cells to transition B cells, transition B cells to mature B cells, and memory B cells. 41 The signaling pathway mediated by the binding of BAFF to BAFFR is essential for the survival and maturation of immature B cells. 42 The nonclassical NF- $\kappa$ B signaling pathway is the main pathway for BAF-F/BAFFR mediated activation. As a matter of fact, the underlying mechanism of the regulation of BAFF-related pathway remains further study.

TRAF2 is a component of the TNF superfamily signaling complex and plays an important role in the regulation and homeostasis of immune cells.<sup>43</sup> It has been reported that TRAF2

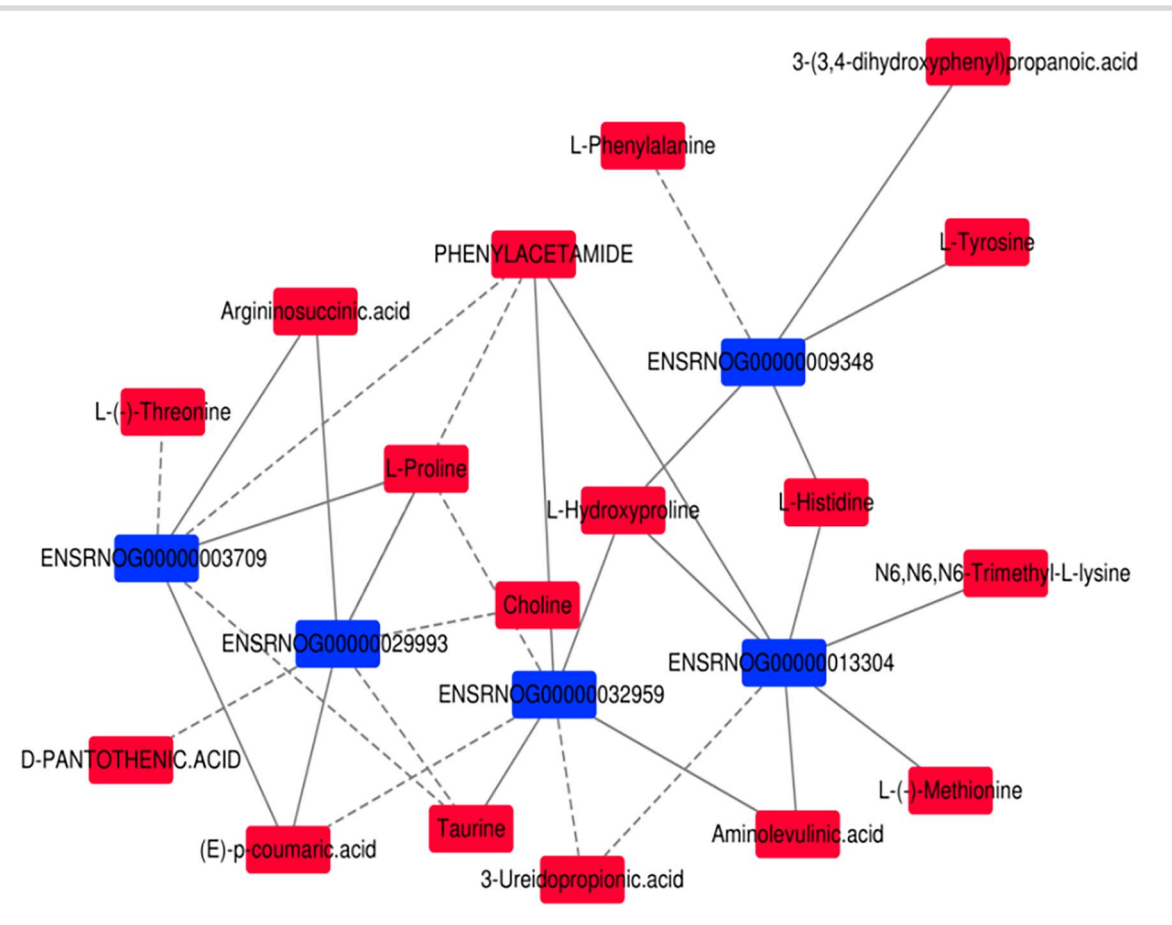


Fig. 10. Correlation network analysis of differential genes and amino acid metabolites. Note: Each line represents the correlation between the gene and the metabolite; the solid line represents a positive correlation and the dashed line represents a negative correlation.

plays an important role in the activation of non-canonical NF- $\kappa$ B and can negatively regulate the non-canonical NF- $\kappa$ B signaling pathway. Previous literature has shown that when TRAF2 is activated, it acts as an intracellular signaling linker molecule and interacts with downstream molecules, recruiting NF-κB transcription factors, activating non-classical NF-κB signaling pathways, and conducting signal transduction, thereby inducing immune and inflammatory responses, promoting the occurrence and development of inflammatory immune diseases. NIK is a key enzyme in the activation of the non-canonical NF- $\kappa$ B signaling pathway.<sup>44</sup> In an alternative NF- $\kappa$ B activation pathway (i.e. non-canonical NF-κB signaling), in the absence of stimulation, NIK binds to the TRAF3/TRAF2/cIAP1/cIAP2 complex that targets its degradation.<sup>45</sup> Following receptor stimulation, the TRAF2/TRAF3/cIAP1/cIAP2 complex accumulates on the receptor, and TRAF2 activation results in the degradation of cIAP1/2 and/or TRAF3.46 This stabilizes cytosolic NIK, leads to massive accumulation and activation of NIK, and allows downstream signaling to activate IKK $\alpha$  and NF- $\kappa$ B2/P100.<sup>46,47</sup> IKK $\alpha$  phosphorylates the NF- $\kappa$ B precursor protein P100, which initiates its partial proteasomal processing to generate the P52 NF- $\kappa$ B subunit. P52 then translocates to the nucleus to activate NF- $\kappa$ B target genes. 44 Additionally, Gardam et al. found that BAFF-BAFFR signaling triggers post-transcriptional depletion of TRAF3 protein through a process that is entirely dependent on TRAF2 expression, thereby reversing TRAF2-TRAF3-mediated repression of survival pathways during B cell development in vivo, suggesting that TRAF2 plays an important role in the regulation of BAFF-BAFFR and downstream signaling pathways, especially in the survival,

activation and function of B cells. 48 The results of this experiment showed that compared with the control group, the simulated lunar dust stimulated the over expression of BAFF in the lung tissue of rats, and the mRNA and protein expressions of BAFFR, TRAF2, NIK, and P52 were increased accordingly. The protein levels of IL-1 $\beta$  and TNF- $\alpha$  were also significantly increased. These results suggest that the simulated lunar dust may promote the occurrence and development of lung inflammation by activating the BAFF/BAFFR-TRAF2-NF-κB signaling pathway, and at the same time cause the disorder of amino acid metabolism.

#### Conclusions

In summary, this study shows that CLDS-i is involved in regulating the activation and differentiation of immune inflammatory cells in rat lung tissue, inducing the activation of inflammation and disease-related signaling pathways, leading to inflammation. The correlation between differential genes and differential amino acid metabolites in rat lung tissue under CLDS-i treatment was obtained by omics combined analysis, and the differential genes involved in amino acid metabolism were screened out. These genes may be the key targets for the treatment of amino acid metabolism diseases. In addition, the results of our experiment suggest that CLDS-i may promote the occurrence and progression of inflammatory response in lung tissue by activating BAFF/BAFFR-mediated NF-κB signaling pathway, and can lead to abnormal amino acid metabolism. However, since the real environment of the moon, such as solar wind and cosmic radiation, cannot be completely simulated on Earth, the toxicity of lunar

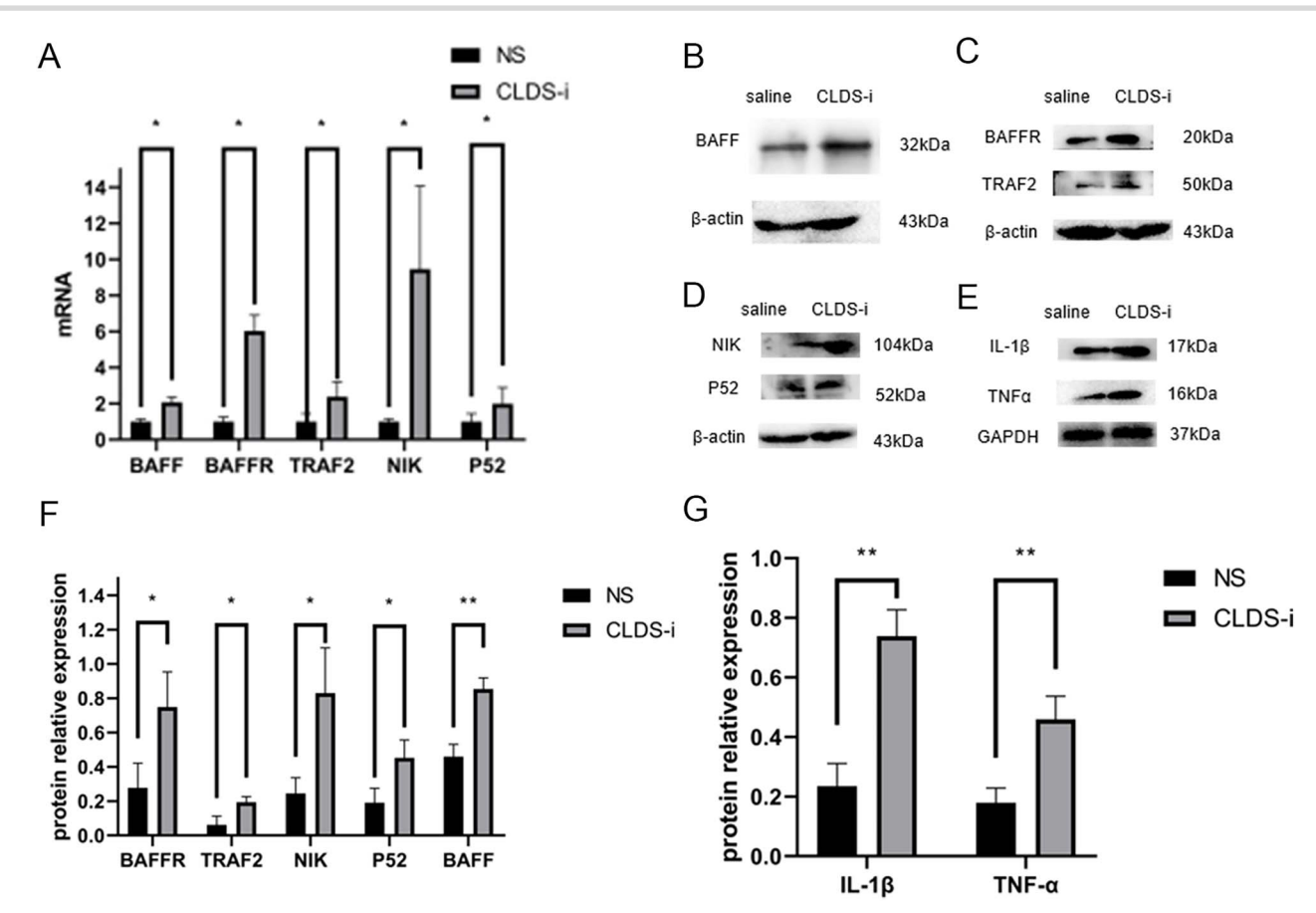


Fig. 11. Relative expression levels of downstream molecules in rat lungs (n = 5). A) BAFF, BAFFR, TRAF2, NIK and P52 mRNA levels in rat lungs. B-E) Western blotting of BAFF, BAFFR, TRAF2, NIK, P52, IL-1 $\beta$  and TNF- $\alpha$  protein. F) The statistics of BAFFR, TRAF2, NIK, P52 and BAFF protein levels in rat lungs. G) The statistics of IL-1 $\beta$  and TNF- $\alpha$  protein levels in rat lungs. Data are presented as mean  $\pm$  standard deviation. Compared with the saline control group, \*P < 0.05, \*\*P < 0.01.

dust under lunar conditions is predicted to be more serious. Our work is to provide reference for astronauts to land on the moon and stay on the moon in the future. In the future, we need to determine the specific components causing toxic effects in lunar dust in the lunar surface environment, further study the mechanism of pneumonic injury caused by exposure to lunar dust and effective therapeutic drugs, and conduct in-depth discussion in more research objects and longer time dimension.

#### **Author contributions**

Sun Y, designed the study, review and supervision. Gu C, performed the experiments, analyzed the data, and wrote the manuscript. Mao MQ, performed the experiments. Liu JG, contributed to the design of the study, review and editing. Li XY, review, editing and supervision. Zhang XP, review and editing. All authors have read and agreed to the published version of the manuscript.

## **Funding**

This study was supported by the Doctoral Scientific Research Fund of Liaoning Provincial Science and Technology Department (20198023), Open Projects Funding of Lunar and Planetary Science Laboratory, MUST—Partner Laboratory of Key Laboratory of Lunar and Deep Space Exploration, CAS (Macau FDCT grant No. 119/2017/A3), the Science and Technology Development Fund

(FDCT) of Macau (0014/2022/A1), and the Science and Technology Research Fund of Shenyang Medical College (20191017).

Conflict of interest statement: There are no conflicts of interest to declare.

#### References

- 1. Calle CI, Buhler CR, McFall JL, Snyder SJ. Particle removal by electrostatic and dielectrophoretic forces for dust control during lunar exploration missions. J Electrost. 2009:67(2-3): 89-92.
- 2. Lam CW, James JT, Latch JN, Hamilton RF Jr, Holian A. Pulmonary toxicity of simulated lunar and martian dusts in mice: II. Biomarkers of acute responses after intratracheal instillation. Inhal Toxicol. 2002:14(9):917-928.
- Park J, Liu Y, Kihm KD, Taylor LA. Characterization of lunar dust for toxicological studies. I: particle size distribution. J Aerosp Eng. 2008:21(4):266-271.
- 4. Taylor L, Pieters C, Patchen A, Taylor DH, Morris R, Keller L, McKay D. Mineralogical characterization of lunar highland soils. Lunar Planet Sci. 2003:XXXIV:1774.
- 5. Hendrix DA, Hurowitz JA, Glotch TD, Schoonen MAA. Olivine dissolution in simulated lung and gastric fluid as an analog to the behavior of lunar particulate matter inside the human respiratory and gastrointestinal systems. Geohealth. 2021:5(11):e2021GH000491.

- 6. Jabbal S, Poli G, Lipworth B. Does size really matter?: relationship of particle size to lung deposition and exhaled fraction. J Allergy Clin Immunol. 2017:139(6):2013-2014.e1.
- 7. Batsura YD, Kruglikov GG, Arutyunov VD. Morphology of experimental pneumoconiosis following inhalation of lunar soil. Bull Exp Biol Med. 1981:92(3):1294-1297.
- 8. Sun Y, Liu JG, Zheng YC, Xiao CL, Wan B, Guo L, Wang XG, Bo W. Research on rat's pulmonary acute injury induced by lunar soil simulant. J Chin Med Assoc. 2018:81(2):133-140.
- 9. An J, Tang W, Wang L, Xue W, Yao W, Zhong Y, Qiu X, Li Y, Chen Y, Wang H, et al. Transcriptomics changes and the candidate pathway in human macrophages induced by different pm(2.5) extracts. Environ Pollut. 2021:289:117890.
- 10. Zhou Z, Qin M, Khodahemmati S, Li W, Niu B, Li J, Liu Y, Gao J. Gene expression in human umbilical vein endothelial cells exposed to fine particulate matter: Rna sequencing analysis. Int J Environ Health Res. 2022:32(9):2052-2064.
- 11. Wang H, Shen X, Liu J, Wu C, Gao J, Zhang Z, Zhang F, Ding W, Lu Z. The effect of exposure time and concentration of airborne pm(2.5) on lung injury in mice: a transcriptome analysis. Redox Biol. 2019:26:101264.
- 12. Shi Y, Zhao T, Yang X, Sun B, Li Y, Duan J, Sun Z. Pm(2.5)induced alteration of DNA methylation and rna-transcription are associated with inflammatory response and lung injury. Sci Total Environ. 2019:650(Pt 1):908-921.
- 13. Liu J, Zhou J, Zhou J, Li M, Chen E, Jiang G, Chen Y, Wu J, Yang Q. Fine particulate matter exposure induces DNA damage by downregulating rad51 expression in human bronchial epithelial Beas-2b cells in vitro. Toxicology. 2020:444: 152581.
- 14. Tang H, Zhang SS, Li XY, Wang SJ, Liu JZ, Li SJ, Li YH, Wu YX. Asic properties and potential application of clds-i lunar dust simulant. Manned Spaceflight. 2017:23:118-122.
- 15. Tang H, Li X, Zhang S, Wang S, Liu J, Li S, Li Y, Wu Y. A lunar dust simulant: Clds-i. Adv Space Res. 2017:59(4):1156-1160.
- 16. Li R, Peng X, Wu Y, Lv W, Xie H, Ishii Y, Zhang C. Exposure to pm(2.5) during pregnancy causes lung inflammation in the offspring: mechanism of action of mogrosides. Ecotoxicol Environ Saf. 2021:228:112955.
- 17. Maleki V, Mahdavi R, Hajizadeh-Sharafabad F, Alizadeh M. The effects of taurine supplementation on oxidative stress indices and inflammation biomarkers in patients with type 2 diabetes: a randomized, double-blind, placebo-controlled trial. Diabetol Metab Syndr. 2020:12(1):9.
- 18. Zhang M, Fu Y, Chen Y, Ma Y, Guo Z, Wang Y, Hao H, Fu Q, Wang Z. Inhibition of the mTORC1/NF-κB axis alters amino acid metabolism in human hepatocytes. Biomed Res Int. 2021:**2021**:8621464.
- 19. van Meijl LE, Popeijus HE, Mensink RP. Amino acids stimulate Akt phosphorylation, and reduce IL-8 production and NF- $\kappa$ B activity in HepG2 liver cells. Mol Nutr Food Res. 2010:54(11): 1568-1573.
- 20. Lim S, Bowen J, Degli-Alessandrini G, Anand M, Cowley A, Levin Prabhu V. Investigating the microwave heating behaviour of lunar soil simulant jsc-1a at different input powers. Sci Rep. 2021:11(1):2133.
- 21. ESA DPO. European space agency news: testing mars and moon soil for sheltering astronauts from radiation. Paris; 2012.
- 22. Wallace WT, Taylor LA, Liu Y, Cooper BL, Mckay DS, Chen B, Jeevarajan AS. Lunar dust and lunar simulant activation and monitoring. Meteorit Planet Sci. 2009:44(7):961-970.
- 23. Zheng Y, Wang S, Ouyang Z, Zou Y, Liu J, Li C, Li X, Feng J. Cas-1 lunar soil simulant. Adv Space Res. 2009:43(3):448-454.

- 24. Lam CW, Scully RR, Zhang Y, Renne RA, Hunter RL, McCluskey RA, Chen BT, Castranova V, Driscoll KE, Gardner DE, et al. Toxicity of lunar dust assessed in inhalation-exposed rats. Inhal Toxicol. 2013:25(12):661-678.
- 25. Sun Y, Liu J, Zhang X, Li X, Zhou B, Lv Z. Mechanisms involved in inflammatory pulmonary fibrosis induced by lunar dust simulant in rats. Environ Toxicol. 2019:34(2):131-140.
- 26. Filho WJ, Fontinele RG, de Souza RR. Reference database of lung volumes and capacities in wistar rats from 2 to 24 months. Curr Aging Sci. 2014:7(3):220-228.
- 27. Song P, Ramprasath T, Wang H, Zou MH. Abnormal kynurenine pathway of tryptophan catabolism in cardiovascular diseases. Cell Mol Life Sci. 2017:74(16):2899-2916.
- 28. Hughes TD, Guner OF, Iradukunda EC, Phillips RS, Bowen JP. The kynurenine pathway and kynurenine 3-monooxygenase inhibitors. Molecules. 2022:27(1):273.
- 29. Harden JL, Lewis SM, Lish SR, Suarez-Farinas M, Gareau D, Lentini T, Johnson-Huang LM, Krueger JG, Lowes MA. The tryptophan metabolism enzyme l-kynureninase is a novel inflammatory factor in psoriasis and other inflammatory diseases. J Allergy Clin Immunol. 2016:137(6):1830-1840.
- 30. Nikolaus S, Schulte B, Al-Massad N, Thieme F, Schulte DM, Bethge J, Rehman A, Tran F, Aden K, Hasler R, et al. Increased tryptophan metabolism is associated with activity of inflammatory bowel diseases. Gastroenterology. 2017:153(6):1504-1516.e2.
- 31. Ala M. Tryptophan metabolites modulate inflammatory bowel disease and colorectal cancer by affecting immune system. Int Rev Immunol. 2022:41(3):326-345.
- 32. Liu R, Evgenov OV, Ichinose F. Nos3 deficiency augments hypoxic pulmonary vasoconstriction and enhances systemic oxygenation during one-lung ventilation in mice. J Appl Physiol. 2005:98(2):748-752.
- 33. Davel AP, Lemos M, Pastro LM, Pedro SC, de Andre PA, Hebeda C, Farsky SH, Saldiva PH, Rossoni LV. Endothelial dysfunction in the pulmonary artery induced by concentrated fine particulate matter exposure is associated with local but not systemic inflammation. Toxicology. 2012:295(1-3):39-46.
- 34. Guo C, Xia Y, Niu P, Jiang L, Duan J, Yu Y, Zhou X, Li Y, Sun Z. Silica nanoparticles induce oxidative stress, inflammation, and endothelial dysfunction in vitro via activation of the MAPK/Nrf2 pathway and nuclear factor-κB signaling. Int J Nanomedicine. 2015:**10**:1463–1477.
- 35. Niedbala W, Alves-Filho JC, Fukada SY, Vieira SM, Mitani A, Sonego F, Mirchandani A, Nascimento DC, Cunha FQ, Liew FY. Regulation of type 17 helper t-cell function by nitric oxide during inflammation. Proc Natl Acad Sci U S A. 2011:108(22):9220-9225.
- 36. Marquezi ML, Roschel HA, Costa AS, Sawada LA, Lancha AH Jr. Effect of aspartate and asparagine supplementation on fatigue determinants in intense exercise. Int J Sport Nutr Exerc Metab. 2003:13(1):65-75.
- 37. Li P, Yin YL, Li D, Woo Kim S, Wu G. Amino acids and immune function. Br J Nutr. 2007:98(2):237-252.
- Sarkar FH, Li Y, Wang Z, Kong D. NF-κB Signaling pathway and its therapeutic implications in human diseases. Int Rev Immunol. 2008:27(5):293-319.
- 39. Zhang LL, Xiao H, Zhang F, Wu YJ, Shu JL, Li Y, Tai Y, Xu SQ, Xu JH, Wei W. BAFF, involved in B cell activation through the NF- $\kappa$ B pathway, is related to disease activity and bone destruction in rheumatoid arthritis. Acta Pharmacol Sin. 2021:42(10):1665-1675.
- 40. Xiao W, Long W, Liu GY, Sui CL, Guo XR, Tian A, Ji CB, Cui XW, Zhang SQ. Molecular cloning, expression and functional analysis of b-cell activating factor (baff) in yellow grouper, epinephelus awoara. Mol Immunol. 2014:59(1):64-70.

- 41. Smulski CR, Eibel H. Baff and baff-receptor in b cell selection and survival. Front Immunol. 2018:9:2285.
- 42. Vincent FB, Morand EF, Schneider P, Mackay F. The baff/april system in sle pathogenesis. Nat Rev Rheumatol. 2014:10(6):365-
- 43. Etemadi N, Chopin M, Anderton H, Tanzer MC, Rickard JA, Abeysekera W, Hall C, Spall SK, Wang B, Xiong Y, et al. TRAF2 regulates TNF and NF- $\kappa$ B signalling to suppress apoptosis and skin inflammation independently of sphingosine kinase 1. elife. 2015:4:e10592. https://doi.org/10.7554/eLife.10592.
- 44. Rapino F, Abhari BA, Jung M, Fulda S. NIK is required for NFκB-mediated induction of BAG3 upon inhibition of constitutive protein degradation pathways. Cell Death Dis. 2015:6(3): e1692.

- 45. Doppler H, Liou GY, Storz P. Downregulation of traf2 mediates nik-induced pancreatic cancer cell proliferation and tumorigenicity. PLoS One. 2013:8(1):e53676.
- 46. Vallabhapurapu S, Matsuzawa A, Zhang W, Tseng PH, Keats JJ, Wang H, Vignali DA, Bergsagel PL, Karin M. Nonredundant and complementary functions of traf2 and traf3 in a ubiquitination cascade that activates nik-dependent alternative nf-kappab signaling. Nat Immunol. 2008:9(12):1364-1370.
- 47. Wajant H, Scheurich P. TNFR1-induced activation of the classical NF-κB pathway. FEBS J. 2011:278(6):862-876.
- Gardam S, Sierro F, Basten A, Mackay F, Brink R. Traf2 and traf3 signal adapters act cooperatively to control the maturation and survival signals delivered to b cells by the baff receptor. Immunity. 2008:28(3):391-401.